ACS APPLIED ENERGY MATERIALS

www.acsaem.org

Forum Article

Controlled Growth of a Photocatalytic Metal−Organic Framework on Conductive Plates by Mixing Direct Synthesis and Postsynthetic Modification Strategies

Guillaume Genesio, Boushra Mortada, Amanda L. Robinson, Jérôme Maynadié, Michaël Odorico, Caroline Mellot-Draznieks, Marc Fontecave, Michaël Carboni,* and Daniel Meyer

Cite This: *ACS Appl. Energy Mater.* 2023, 6, 9188−9195

Read Online

ACCESS | Metrics & More | Article Recommendations | Supporting Information

ABSTRACT: In this work, we develop a two-step process for the controlled growth of a thin layer of a functionalized and photosensitive metal−organic framework (MOF), namely Ru−Ti−UiO-67, on the surface of a plate coated with indium tin oxide (ITO), a transparent conductive oxide (TCO). In the first step, the *in situ* controlled growth of a layer of UiO-67-based MOF doped with a photosensitizer (ruthenium complex), herein referred to as Ru−UiO-67, is carried out on the surface of the ITO-coated plate, leading to Ru−UiO-67/ITO. The obtained MOF layer is relatively thin, allowing increased interactions between the MOF material and the TCO surface, and consists of crystals in the near-nanometer particle size. In the second step, a postsynthetic modification (PSM) process is applied to Ru−UiO-67/ITO to integrate Ti catalytic sites into the MOF framework, leading to Ru−Ti−UiO-67/ITO (containing both the photosensitizer and catalyst) while maintaining the MOF's structure and morphology in addition to its strong interaction with the substrate. Importantly, on the synthetic level, this work demonstrates the possibility to form a homogeneous surface anchored with MOF on a transparent conductive surface, whereby the obtained MOF layer is strongly bound to the substrate and postsynthetic chemical modifications are enabled without any loss of material. Furthermore, the obtained material is proven to exhibit an efficient visible-light-driven photodegradation activity in aqueous solution.

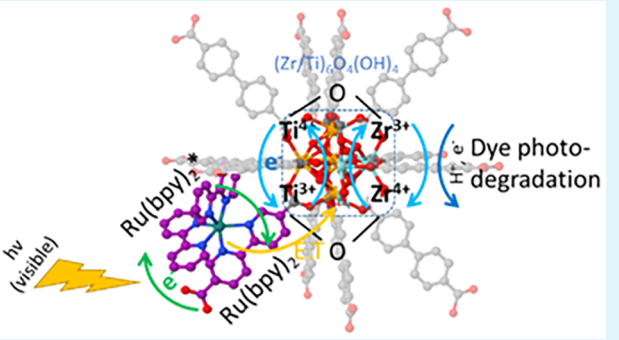

KEYWORDS: *Metal−organic framework, controlled growth, catalytic, photoactive, epitaxial*

INTRODUCTION

Metal−organic frameworks (MOFs), or hybrid porous organic−inorganic materials, are a class of crystalline solids obtained by the self-assembly of organic ligands (linkers) with metal ions or clusters.[1,2] These materials are attractive for their exceptional properties, such as their large porosity and high surface areas, in addition to their chemical and thermal stabilities.[3] Moreover, their tailorable design, attributed to the wide variety of available organic linkers and metals, has led to their potential application in different domains such as gas storage,[4] heterogeneous catalysis,[5] extraction,[6] metal separation,[7] drug delivery,[8,9] and photocatalysis.[10,11]

Recently, there has been a growing interest in the development of photocatalytically active MOF materials for solar energy conversion/storage applications (e.g., water splitting or CO_2 reduction) in the visible spectrum of light. To this end, the photocatalytic activity of several MOF materials has been explored, where promising results have been obtained in the domains of photodegradation of organic pollutants and CO_2 reduction.[12−16] Among the most interesting results are those obtained with a modified Zr-MOF, UiO-67 (based on a biphenyl dicarboxylic acid (BPDC) ligand), which is known for its high chemical and thermal stabilities, in addition to its ability to accommodate different isostructural linkers, metals, or defects in its structure.[17] Of note, because it is possible to dope the UiO-67 MOF structure with transition metal complexes, based on Ir, Re, or Ru ions bound to a bipyridine dicarboxylic acid (BPyDC) ligand, and, thus, to add a "light antenna", there have been many reports in the literature[18−20] of materials that have been efficient for the photocatalytic reduction of CO_2, and optical and photocatalytic properties have been reported.

Special Issue: Metal-Organic Frameworks for Energy Storage Applications

Received: February 17, 2023
Accepted: May 15, 2023
Published: June 1, 2023

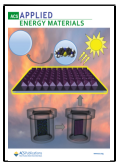

Scheme 1. Two-Step Strategy Applied for the Synthesis of Photocatalytic Ru−Ti−UiO-67 on a TCO Plate Involving the *In Situ* Solvothermal Growth of Ru−UiO-67 MOF Followed by PSM

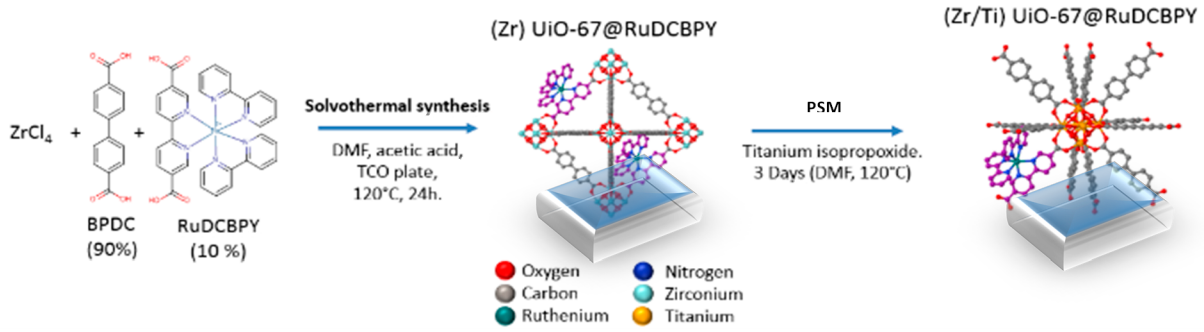

Thus, the use of heterometallic MOFs is of particular interest in the domain of photocatalysis, as these materials can accommodate in their structure both a light antenna and a catalyst.[21] More specifically, integrating different ligands and metals into the MOF structure can be achieved during the MOF synthesis (*in situ*); however, it can also be accomplished following a postsynthetic modification strategy (PSM).[22] In order to overcome the inert redox nature of Zr(IV) while benefiting from the exceptional chemical stability of Zr-based oxo-clusters, the development of heterometallic Ti/Zr-oxo clusters in MOFs has recently gathered increasing interest as recently reviewed.[23] Typically, Liu et al. reported the introduction of Ti(IV) in UiO-66 via the formation of oxo-bridged hetero-Zr−Ti clusters allowing a photocatalyst efficient in the UV spectrum of light.[24] While the incorporation of Ti(IV) metal centers into the inorganic subnetwork of NH_2−UiO-66 has been recurrently reported to enhance photocatalytic performances,[25−27] the possibility of forming supported TiO_2 nanoparticles rather than performing a Zr/Ti exchange when using PSM strategies has been also reported in UiO-66.[28] Overall, these postsynthetic modifications to form Ti/Zr-containing MOFs highlight the possibility of functionalizing the MOF material for enhanced photocatalytic applications. Also, the UiO-type material's frontier orbitals are known to be defined by a ligand−ligand transition whereby a possible modulation of photocatalytic properties is allowed upon the incorporation of Ti.[29,30]

In this regard, our group had already reported the synthesis of a MOF material that combines both a light harvesting antenna (on the linker) and a catalytic site (on the metal node), thus acting as a multifunctional MOF.[11] A ruthenium complex, acting as a photoactive linker, was introduced during the MOF synthesis, and then, a PSM route was followed to exchange up to 50% of the Zr atoms in the metal nodes with Ti. Charge transfer between the light antenna and the catalytic site was proven through the photodegradation of a simulant organic pollutant (methylene blue).[11] Nevertheless, up to this point, such systems have only been produced in the form of powders; thus, the possibility to recover and recycle them is limited. To overcome these limitations and enhance the material's performance, we have therefore turned our focus to the growth of MOFs as films on the surface of a support. Among the different supports on which MOF films can be grown, glass substrates coated with a layer of transparent conductive oxides (TCOs), mainly indium tin oxide (ITO) and fluorine tin oxide (FTO), are of particular interest for photocatalytic and electro-photocatalytic applications.[31−33] To the best of our knowledge, despite the large number of MOF/TCO systems reported in the literature,[34,35] PSM strategies on MOF/ITO systems have been scarcely reported for photocatalytic purposes, which is mainly due to the difficulty of controlling the morphology of the MOF layer formed on the surface of the substrate. The first difficulty with such strategies is to have MOF particles that are attached to the ITO surface well enough so that they survive postsynthetic chemistry without alteration of the whole MOF/ITO system. The second critical point is the difficulty of analyzing the MOF solid immobilized in the MOF/ITO system when compared to the easy-to-characterize MOF powder. Even though different techniques have been proposed to develop such films, direct *in situ* growth by solvothermal synthesis is among the simplest and one of the most highly efficient approaches. It involves placing the support in the bulk solution containing all the reactants (metal salt and organic linker) and the solvent in the same reactor. The reaction mixture is then heated (where the reaction temperature and duration vary according to the specific MOF synthesis protocol), and the MOF material grows directly on the surface of the substrate forming a film. Morris et al. used this strategy to form a Ru-doped UiO-67 MOF layer on the surface of a FTO plate.[36] In this case, prior to the solvothermal synthesis, the substrate was prefunctionalized by depositing a layer of the linker on its surface, in a process known as the surface-anchored monolayer (SAM), in the aim of facilitating the MOF nucleation and increasing the binding strength between the MOF and the FTO surface. However, this resulted in the formation of a relatively thick layer containing numerous cracks. In another study, the surface of the FTO was coated with a layer of TiO_2, on top of which the MOF film was grown.[37] It was found that although the TiO_2 layer did indeed enhance the electron transfer from the MOF to the FTO, the targeted MOF film morphology could, nevertheless, not be obtained. Other methods have also been developed for growing a UiO-67 MOF, including a photocatalytic component, on TCO substrates using Ru(bpy)(tpy)-(H_2O)DCBPY, which is efficient for water reduction.[38,39] A couple of other studies have been reported, but more works are needed for the synthesis of MOF/TCO systems allowing a better control of the morphology, the stability, and the homogeneity of the deposited film.

Herein, we propose a unique two-step process for the synthesis of functionalized and photocatalytically active UiO-67 MOF on the surface of an ITO-coated plate. Using acetic acid as a modulator and by controlling the concentrations of the metal and organic precursors, the developed process allows, in the first step, the *in situ* controlled growth of a thin layer of a photoactive UiO-67 MOF material doped with

https://doi.org/10.1021/acsaem.3c00447
ACS Appl. Energy Mater. 2023, 6, 9188−9195

$Ru(bpy)_2DCBPY$, denoted in this work as Ru−UiO-67/ITO (Scheme 1). In the second step, the MOF material that was adhered to the surface of the substrate is further functionalized by introducing a catalytic Ti ion into its structure (Scheme 1), through a PSM reaction, with the obtained material denoted as Ru−Ti−UIO-67/ITO. The photocatalytic activity of the MOF/ITO systems is then evaluated through the degradation of an organic pollutant (methylene blue).

EXPERIMENTAL SECTION

Among the different methods that have been developed for the synthesis of MOF thin films, the direct solvothermal synthesis remains the most extensively applied. In our case, we chose to use this synthesis method, as it is timesaving and allows obtaining the Ru-doped material in a single step, instead of going through two separate steps (synthesis of UiO-67 followed by doping with Ru). Moreover, this technique allows control over the crystal size and morphology. For instance, herein, by employing a modulator and decreasing the concentration of the metal precursor, crystals of relatively small particle size could be obtained. Smaller crystals can also contribute to thinner films, which are highly desired in photocatalysis, unlike the evaporation and electrochemical deposition methods that can lead to the formation of thick layers. The obtained MOF crystals in the case of the solvothermal synthesis were strongly adhered to the ITO surface through a chemical bond and not just deposited on the surface, which was demonstrated by their resilience to washing with organic solvents and/or by exposing them to ultrasound irradiation through sonication and further proven with AFM analysis. However, this is not the case for the evaporation method, for example, where the obtained MOF materials are only loosely deposited on the surface of the plate.

All the reagents were purchased from Sigma-Aldrich and used as received. One-side-coated ITO plates were purchased from Solems (France). UV−visible analyses for the Ru complex (3) and the UIO-67@Ru/ITO were recorded on a Shimadzu UV-36000 UV−vis−NIR spectrometer with a diffuse reflectance measurement system. The Ru complex was suspended in acetonitrile, whereas the MOF material synthesized on the ITO-coated plate was analyzed directly without any further modification. Grazing incidence and powder XRD patterns were obtained with a Bruker D8 Advance diffractometer, using CuKα radiation (λ = 1.5418 Å). In the case of grazing incidence XRD, the incident angle was fixed at 0.2°. SEM images were acquired with an FEI Quanta 200 environmental scanning electron microscope, equipped with an Everhart-Thornley Detector (ETD), and a backscattered electron detector (BSED) was used to record images with an acceleration voltage of 10 kV under high vacuum conditions. The chemical compositions of the solutions were determined with ICP-AES (Spectro Acros from Ametek). Prior to the analyses, MOFs were digested in a piranha solution, consisting of 125 μL of sulfuric acid and 75 μL of hydrogen peroxide, by heating at 120 °C for 2h. This was followed by diluting a certain volume of the digested MOF solution in nitric acid (2%). We note that no MOF reprecipitation was observed after the acid digestion.

The paragraphs below summarize the protocols for the synthesis of the MOF on ITO-coated plates and the PSM with Ti. Nevertheless, details on the synthesis conditions and characterization of complexes and ligands are provided within the ESI.

MOF Film Synthesis. Prior to the MOF synthesis, the ligand $Ru(bpy)_2(bpydc)$ was prepared following the protocol reported by Xie et al. (see SI for synthesis protocols). The Ru−UiO-67 on ITO was obtained by direct growth on the surface of the untreated ITO plate (2.5 × 1 cm) through solvothermal synthesis. The synthesis involved placing the substrate vertically in a vial containing $ZrCl_4$ anhydrous (3 mg), the ligands, H_2bpdc (2.86 mg) and $Ru(bpy)_2(bpdc)$ (0.78 mg), dissolved in pure *N*,*N*-dimethylformamide (DMF, 0.03% H_2O) (7 mL), and acetic acid as a modulator (0.5 mL). The molar composition of the reaction mixture is 1 Zr:1 ligands:680 acetic acid:7000 DMF. It is important to note that it was proven that placing the substrate in a vertical position in the reaction medium during the solvothermal synthesis results in the formation of a homogeneous MOF layer on the surface and prevents the agglomeration of crystals, which was not the case when the plate was placed in a slightly inclined position (an inhomogeneous layer with agglomerated MOF crystals was obtained). The reaction medium was heated to 120 °C for 24 h. The plate was later rinsed with DMF (once) and with ethanol (EtOH) (twice) in order to remove any reactant residues and then dried at 40 °C for a few hours.

In order to determine the face of the plate coated with ITO, the conductivity of the plate was measured with a multimeter. It is important to note that the synthesis of UiO-67/ITO was carried out following the same protocol as Ru−UiO-67/ITO, however, without the addition of the Ru complex and by using 3 mg of H_2bpdc.

MOF powder formed in the bulk medium (in the case of both UiO-67/ITO and Ru−UiO-67/ITO), due to the presence of excess reactants, was recovered by sonication, followed by centrifugation (10 000 rpm, 2 min), and washed with DMF and then with EtOH. Based on XRD and SEM analyses (Figure S8), respectively, this powder was proven to have a similar structure and morphology as the MOF material anchored on the surface of the ITO-coated plate. It is important to note that this MOF residue was used to determine the chemical composition of Ru−UiO-67 and Ru−Ti−UiO-67 through ICP analyses, as it is not possible to digest the MOF layer on the ITO plate.

PSM of Ru−UiO-67/ITO. The PSM step involved washing the Ru−UiO-67/ITO obtained via the direct growth solvothermal synthesis only with DMF and then placing the TCO plate in a vial containing a solution of titanium isopropoxide in anhydrous DMF. It is important to note that the PSM reaction was realized under inert conditions (under argon flow) in a glovebox, in order to limit the decomposition of titanium isopropoxide through hydrolysis. Herein, a 1:1 Zr:Ti molar ratio was used, and the plate was suspended in the titanium isopropoxide in anhydrous DMF mixture for 3 days at 120 °C (Zr/Ru/Ti ratio has been already optimized in our previous work[11]). The obtained material on the surface of the plate was then washed thoroughly with DMF and EtOH and dried under air.

RESULTS AND DISCUSSION

MOFs were prepared on the surfaces of ITO plates following a solvothermal synthesis protocol that involved placing the ITO plate vertically in the bulk solution containing the metal and organic precursors dissolved in an organic solvent and in the presence of acetic acid as a modulator. The synthesis of UiO-67/ITO and Ru−UiO-67/ITO is detailed in the Experimental Section. It is important to note that the strong adhesion of the materials to the substrate's surface was demonstrated by their resilience to washing with organic solvents and/or by exposing them to ultrasound irradiation through sonication.

In order to confirm the formation of the desired MOF structure, Ru−UiO-67/ITO was analyzed with grazing incidence X-ray diffraction at an incident angle of 0.3°. The obtained XRD pattern is represented in Figure 1, which in the purpose of comparison also represents the theoretical XRD pattern of powder UiO-67 and that of Ru−UiO-67 powder (synthesized by referring to the protocol reported by Amador et al.).[11] We note that the latter was obtained through powder X-ray diffraction (PXRD) analysis. Figure 1 shows that the XRD patterns obtained for the different materials are similar and indeed correspond to the UiO-67 structure. Based on scanning electron microscopy (SEM) analysis, at high magnification, it can be observed that the Ru−UiO-67 crystals grown on the surface of the plate possess an octahedral morphology, which is the typical morphology of UiO-67 (Figure 2). It was observed that almost all crystals exposed the same crystallographic faces, which is probably related to preferential growth.

https://doi.org/10.1021/acsaem.3c00447
ACS Appl. Energy Mater. 2023, 6, 9188−9195

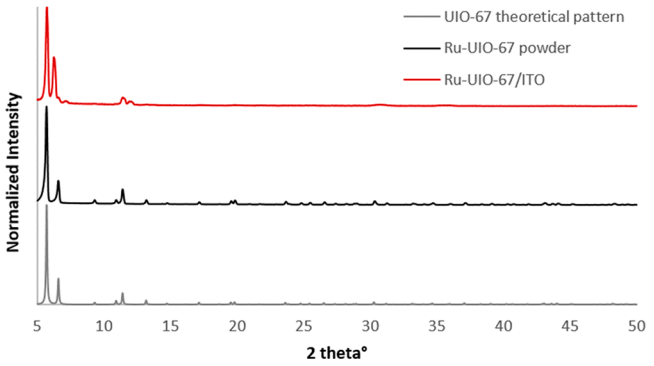

Figure 1. XRD patterns of Ru−UiO-67 powder and Ru−UiO-67 on ITO-coated plates (Ru−UiO-67/ITO). For comparison, the theoretical XRD pattern of UiO-67 is also presented.

Furthermore, the low magnification images reveal a homogeneous distribution in size and crystal density all over the film's surface. The crystal size is around 1 μm, and the surface coverage by MOF crystals is estimated at 56% (based on SEM analyses). Indeed, the relatively small particle size (~1 μm) exhibited by the Ru−UiO-67 crystals grown on the surface of the ITO-coated plate can be attributed to the use of acetic acid as a modulator and to the decrease in the concentration of the metal precursor during the synthesis. SEM images were also recorded while tilting the detector by an angle of 75° (Figure S1). The obtained results reveal that although the MOF on the surface presents a slightly concaved shape (probably due to the drying process), the UiO-67 morphology is well maintained.

Atomic force microscopy (AFM) analyses were performed in the aim of investigating the possible formation of a junction between the substrate and the MOF crystals (Figure 3). This technique also allows the study of the topology of the crystal surface at very high resolution that can reach up to several nanometers. Indeed, the 3D image represented in Figure 3a clearly shows the MOF/ITO junction. Moreover, the roughness obtained for the surface MOF crystals (~4 nm) is lower than the value registered for the substrate (~15 nm). A difference in roughness at the interface between the MOF layer and the ITO plate was also determined with AFM analysis. For instance, the MOF layer present on the surface of the ITO plate was scraped (with the aid of the tip of the cantilever), and the roughness of the underlying layer was determined. A value of 9 nm was obtained, compared to 15 nm for the nongraphed ITO surface. This indicates that the ITO surface was altered during the growth of the MOF crystals and further confirms the formation of a chemical bond between the plate's surface and the MOF material. Furthermore, Figure S2 clearly shows the presence of traces of octahedral MOF crystals remaining on the surface of the ITO plate that could not be removed using the tip of the cantilever. These features can be considered as indications of the presence of a strong chemical interaction between the surface of the ITO plate and the Ru−UiO-67 crystals, as a result of the growth of the MOF on the plate's surface. Roughness profiles were also recorded with AFM analysis. The profiles were realized on a nanometric scale over six sections of 250 nm on the exposed face of the crystal. The interpretation of the obtained roughness profiles indicates that a face is constituted of multiple facets separated by a distance of 1.6 nm, which is in agreement with the value of 1.56 nm corresponding to d(111) in the UiO-67 crystal structure (Figure 3b). This also confirms the preferential orientation of the crystals on the surface of the ITO plate in the [111] direction.

Inductively coupled plasma atomic emission spectroscopy (ICP-AES) analysis was carried out on the powder MOF material recovered from the bulk solution (as it is not possible to analyze the MOFs grown on the TCO plates using this technique), mainly with the aim of determining the amount of Ru (Ru complex). Based on the results obtained for the digested material, the proposed formula of the Ru-doped MOF material is as follows: $Zr_6O_4OH_4(bpdc)_{5.6}[Ru(bpy)_2bpdc)]_{0.4}$.

The presence of ruthenium in Ru−UiO-67 was also confirmed with UV−vis spectroscopy analysis, and the obtained results were compared to those of $Ru(bpy)_2bpdc$ in solution as a reference (Figure S3). The UV−vis spectrum reveals a maximum absorbance peak at 450 nm in Ru−UiO-67, which is characteristic of the Ru complex. Moreover, fluorescence emission spectroscopy was also carried out in the aim of proving the functionalization of UiO-67 with Ru. To this end, a sample of Ru−UiO-67 was excited by irradiation with a light source of a wavelength of 450 nm (the absorption wavelength of Ru). The obtained results for Ru−UiO-67/ITO reveal a significant peak around 640 nm, which is characteristic of Ru and can be attributed to the photon emitted upon the relaxation of the Ru atom (Figure S4).

Integration of the Ti Catalyst: Postsynthetic Modification of Ru−UiO-67/ITO. In order to study the possibility of functionalizing such a MOF film, Ti catalytic sites were inserted into the Ru−UiO-67 MOF material deposited on the

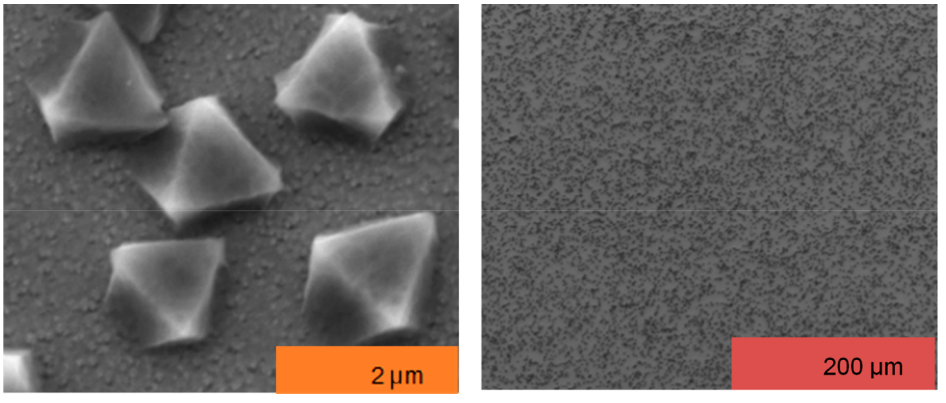

Figure 2. SEM images of Ru−UiO-67/ITO at two different magnifications: top 10 000× and bottom 250×.

https://doi.org/10.1021/acsaem.3c00447
ACS Appl. Energy Mater. 2023, 6, 9188−9195

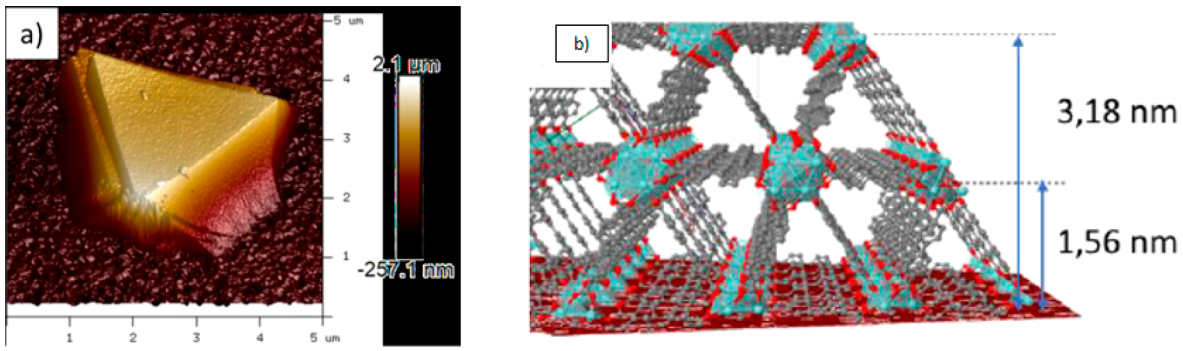

Figure 3. AFM pictures of Ru−UiO-67 crystals on the ITO substrate (a) and roughness profile of the surface of the crystal and crystal structure representation (b).

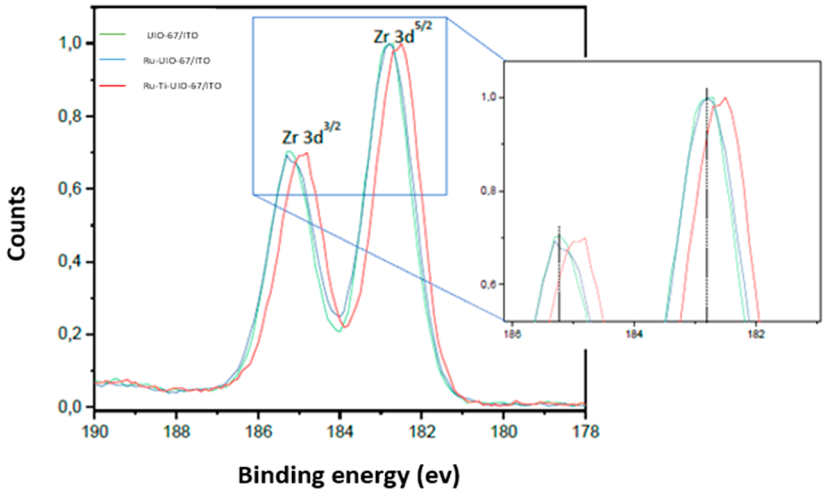

Figure 4. XPS analyses of Zr 3d of UiO-67, Ru−UiO-67, and Ru−Ti−UiO-67.

surface of the ITO plate in a second reaction step, known as PSM. Theoretically, the Ti catalytic sites can be either present in the MOF pores in the form of TiO_2 nanoparticles or may be incorporated at the metal nodes. The conditions for PSM involved placing Ru−UiO-67/ITO in a solution of titanium isopropoxide in anhydrous DMF under inert atmosphere. This was followed by heating the reaction mixture at 120 °C for 3 days. After washing thoroughly with DMF and EtOH, the material was then dried in air. Herein, the Ti-functionalized material obtained after PSM on the surface of the ITO plate is denoted as Ru−Ti−UiO-67/ITO.

The obtained material was analyzed with SEM, which revealed that the MOF film was still attached to the plate's surface, with an estimated MOF surface coverage around 56% (Figure S5) and that the morphology of the MOF crystals was not modified.

Moreover, according to Figure S6, the XRD patterns of the Ru−UiO-67/ITO (Ti-free) and Ru−Ti−UiO-67/ITO (Ti-containing) MOF materials are similar, indicating that the PSM step did not alter the crystallinity of the MOF material. In Ru−UiO-67/ITO, an additional peak of impurity is observed at 6.2 2θ that is eliminated during the PSM process. After PSM, the Ti:Zr ratio was determined to be 1:1, based on ICP-AES measurements. It is important to note that by referring to the experimental results that were previously reported by Navarro Amador et al.,[11] this percentage does not increase on using higher titanium isopropoxide concentrations or on increasing the duration of the PSM reaction. ICP-AES results also proved that the percentage of ruthenium was not affected after PSM and remained around 4%. On the other hand, the fluorescence lifetime measurement revealed a slight shift from 750 to 595 ns (Figure S7), which might be attributed to a charge transfer between Ru and Ti within the cluster (among other phenomena) that quenches partially the fluorescence of Ru, whereas the photoluminescence and the optical adsorption do not change when compared to that of Ru−UiO-67/ITO as previously reported on powder state.[11]

X-ray photoelectron spectroscopy (XPS) analysis is a technique that gives information on the chemical environment surrounding the elements constituting a certain material. Therefore, following the PSM step, XPS analyses were performed mainly with the aim of confirming the incorporation of Ti in the MOF structure while following the changes in the chemical environment of surrounding Zr.

Figure 4 reveals that after PSM, the two peaks initially present in Ru−UiO-67 at 182.7 (Zr 3d 5/2) and 185.2 ev (Zr 3d 3/2) are shifted to lower binding energy values in the Ru−Ti−UiO-67 MOF. In line with a previous report, such shifts result from an enhanced electron density around Zr occurring in oxo-bridged Zr−Ti clusters.[26] Furthermore, a similar shift is also observed when the analysis is performed at depths of 10 and 60 nm in the sample, indicating that this phenomenon does not only occur on the surface of the crystals but also deep within the MOF framework. It is important to note that the presence of Ru in Ru−UiO-67 could not be detected with XPS, probably due to its low atomic concentration.

https://doi.org/10.1021/acsaem.3c00447
ACS Appl. Energy Mater. 2023, 6, 9188−9195

Furthermore, Figure S9 represents the XPS spectra of Ti recorded on the surface of Ru−Ti−UiO-67/ITO (at 0 nm) and at 10 and 60 nm deep into the MOF film (after being irradiated with a laser). The obtained results reveal the presence of two peaks at 458.7 and 464.3 eV. Indeed, the three obtained spectra are superimposable, which indicates the homogeneous distribution of Ti atoms throughout the sample and that they all exhibit the same oxidation state and surrounding environment. The XPS profile of Ti in Ru−Ti−UiO-67/ITO resembles that of Ti in TiO_2 reported by Zhu et al.,[40] which indicates that Ti present in both materials exhibits the same oxidation state of IV. However, the peaks in the XPS spectrum of Ti in Ru−Ti−UiO-67/ITO are shifted to lower binding energy values (458.7 and 464.3 eV) when compared to those of Ti in TiO_2 nanoparticles[40] (459.5 and 465.2 eV) while being close to those reported in the UiO-66(Ti) MOF (458.1 and 463.8 eV).[24] Thus, the Ti atoms present in Ru−Ti−UiO-67/ITO do not correspond to TiO_2 nanoparticles, and the shift toward lower binding energy values in Ru−Ti−UiO-67/ITO may be rather assigned to Ti−O−Zr bonds and, thus, to Ti atoms incorporated in the cluster of Ru−Ti−UiO-67/ITO following the PSM step. Moreover, in our previous study (similar strategy on MOFs powder[11]), the porosity of the MOFs before and after Ti treatment is very similar, suggesting that Ti is bound to the cluster and not inside the cavity as TiO_2 particles.

Ru−Ti−UiO-67/ITO for the Photodegradation of Methylene Blue (MB). In order to investigate the photocatalytic activity of the Ru−Ti−UiO-67/ITO system, the photodegradation of methylene blue (MB), an organic dye pollutant, was carried out as a proof of concept. Prior to the photodegradation test, the Ru−Ti@UiO-67/ITO plate was placed in a MB solution of 1.5 mg/L for 12 h in the absence of light so as to allow the adsorption of the dye within the MOF material. Then, the photocatalytic activity of Ru−Ti−UiO-67/ITO was evaluated by irradiating the reaction medium with visible light (λ>420 nm) in a Rayonet RPR-100n Photochemical Reactor ($P \approx 400$ W). The concentration of MB remaining in the solution at the end of the photocatalytic test was determined through UV−visible spectroscopy analyses. The photodegradation of MB was also studied using UiO-67/ITO, Ru−UiO-67/ITO, and Ti-UiO-67/ITO, whose photocatalytic activities were compared to that of Ru−Ti−UiO-67/ITO.

Figure 5 shows the variation of the dye concentration as a function of the irradiation time for all the studied systems. As expected, Ru−UiO-67/ITO exhibited a similar activity for MB degradation than the bare support ITO or the UiO-67/ITO system, confirming that the Ru centers in Ru−UiO-67/ITO do not possess any significant catalytic activity. By contrast, the enhanced degradation of MB when using Ti-UiO-67/ITO points toward the catalytic role of Ti in this system for the dye's photodegradation. Consistently, among all the studied systems, both the Ti-UiO-67/ITO and Ru−Ti−UiO-67/ITO composite systems were the most active ones as photocatalysts, exhibiting the lowest dye concentrations after 6 h of irradiation (Figure 5).

Thus, the combination of both the photosensitizer (Ru) and photocatalyst (Ti), as in the case of Ru−Ti−UiO-67/ITO, enhances the photoactivity of the system and kinetics of degradation of the dye molecule, respectively, when compared to the systems missing one of the two components or both. This is supported by the known photosensitive role of titanium, in addition to its catalytic role, as previously proven by Wang et al. in the case of the UiO-66(Ti) system.[24]

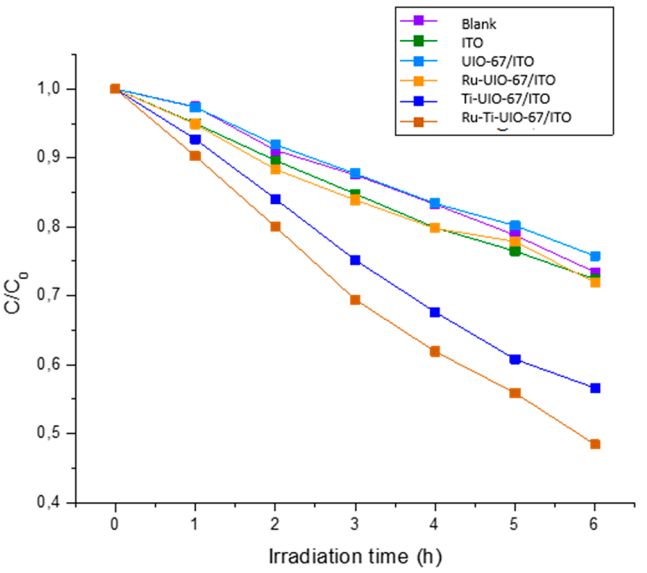

Figure 5. Photodegradation of MB represented by the variation of normalized concentration of MB vs irradiation time under visible-light (λ > 420 nm), using a blank, unmodified ITO-coated plate and UiO-67 derivatives on ITO-coated plates.

Such enhanced activity of the Ru−Ti−UiO-67/ITO system might result from the ligand-to-cluster charge transfer phenomenon taking place between the photosensitizer and the catalyst (Ru complex and Ti, respectively). Also, it is important to note that the Ru−Ti−UiO-67/ITO system exhibits a significantly enhanced photocatalytic activity for MB degradation when compared to that of the same powder system reported by Amador et al.[11] Illustratively, the percentage of MB degradation after 3.5 h of illumination reaches 80% when using 5 mg of Ru−Ti−UiO-67 powder, whereas only 0.01 mg of MOF deposited on the surface of the ITO plate in the Ru−Ti−UiO-67/ITO system allows reaching 35% MB degradation. Although the Ru−Ti−UiO-67/ITO system suffers from lower quantities of catalyst deposited on the ITO plate with respect to those used in suspension, the Ru−Ti−UiO-67/ITO system leads to a much more efficient exposure of the crystallites to light. This may rationalized by the optimal orientation and robust immobilization of the MOF crystallites on the surface of the ITO plate (Figure 3), which allows a better exposure of the whole photocatalytic system to light during the experiment, unlike the case of the MOF powder in suspension, the latter being in constant motion (due to stirring) and, hence, randomly exposed to light and subject to light diffusion by the suspension.[41] Finally, the recyclability of the Ru−Ti−UiO-67/ITO system was studied over three catalytic cycles. The results are presented in Figure 6 and reveal that the photocatalytic activity after 6 h of irradiation remains identical over the three cycles. These results are promising and confirm the advantage of MOF films over powder samples in terms efficiency, recovery and potential reusability during photocatalysis.

CONCLUSION

Herein, an ITO plate was successfully functionalized with photocatalytic MOFs via a unique two-step strategy. The latter involves in the first step the controlled growth of a thin layer of

https://doi.org/10.1021/acsaem.3c00447
ACS Appl. Energy Mater. 2023, 6, 9188−9195

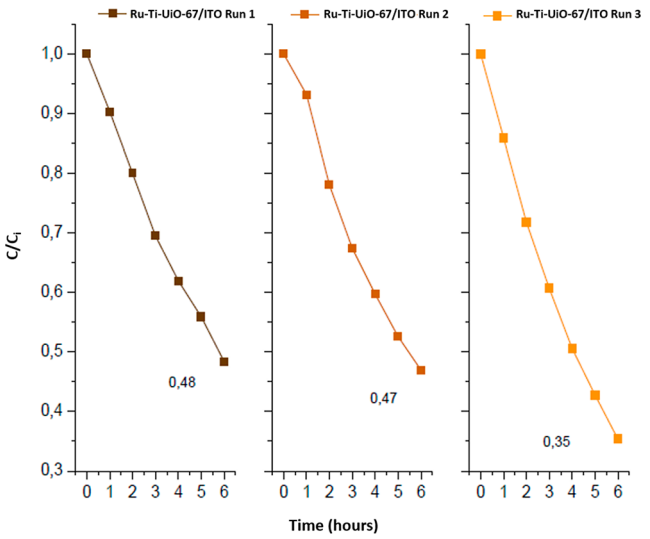

Figure 6. Photocatalytic activity of the Ru−Ti−UiO-67/ITO system over three cycles/runs.

Ru−UiO-67 on the surface of the ITO substrate using acetic acid as a modulator. Structural analysis realized on the obtained MOF film revealed the formation of a homogeneous layer consisting of octahedral crystals near nanometers in size, with no intergrown MOF crystals. In the second step, and by virtue of the strong bonding between the MOF film and the surface of the substrate, it was also possible to introduce catalytic species into the MOF structure, through a PSM reaction performed on the MOF film, without altering the MOF structure and morphology or compromising the strong MOF−substrate bonding. The resulting Ru−Ti−UiO-67/ITO system was shown to be highly efficient in the photodegradation of methylene blue, with an enhanced activity compared to the unmodified ITO substrate and the MOF/ITO systems lacking the photosensitizer and/or the catalyst. With the long-term goal to develop robust and recyclable heterogeneous noble metal-free photosystems in the field of energy, the present work shows that Ru−Ti−UiO-67 deposited on ITO offers a clear benefit in terms of catalytic efficiency while allowing integration of photocatalysts into easy-to-use devices. We believe this work will inspire the use of similar strategies to design new photocatalytic systems deposited on transparent and conductive supports.

■ ASSOCIATED CONTENT

Supporting Information

The Supporting Information is available free of charge at https://pubs.acs.org/doi/10.1021/acsaem.3c00447.

Synthesis of the Ru complexes, characterization of the MOF materials (SEM and AFM of Ru−UiO-67/ITO, UV−visible and fluorescence emission of Ru−UiO-67/ITO, SEM images of the Ru−Ti−UiO-67/ITO, XRD patterns of Ru−UiO-67/ITO and Ru−Ti−UiO-67/ITO, fluorescence emission lifetime of Ru−UiO-67/ITO and Ru−Ti−UiO-67/ITO, SEM image of the Ru−UiO-67, XPS analyses of Ti 2p3 of Ru−Ti−UiO-67/ITO (PDF)

■ AUTHOR INFORMATION

Corresponding Author

Michaël Carboni − *ICSM, CEA, Univ Montpellier, CNRS, ENSCM, 30207 Marcoule, France;* orcid.org/0000-0003-0855-9354; Email: Michael.carboni@cea.fr

Authors

Guillaume Genesio − *ICSM, CEA, Univ Montpellier, CNRS, ENSCM, 30207 Marcoule, France*

Boushra Mortada − *ICSM, CEA, Univ Montpellier, CNRS, ENSCM, 30207 Marcoule, France*

Amanda L. Robinson − *Collège de France, Laboratoire de Chimie des Processus Biologiques, UMR 8229. CNRS, Sorbonne Université, 75231 Paris Cedex 05, France*

Jérôme Maynadié − *ICSM, CEA, Univ Montpellier, CNRS, ENSCM, 30207 Marcoule, France*

Michaël Odorico − *ICSM, CEA, Univ Montpellier, CNRS, ENSCM, 30207 Marcoule, France*

Caroline Mellot-Draznieks − *Collège de France, Laboratoire de Chimie des Processus Biologiques, UMR 8229. CNRS, Sorbonne Université, 75231 Paris Cedex 05, France;* orcid.org/0000-0003-3670-4600

Marc Fontecave − *Collège de France, Laboratoire de Chimie des Processus Biologiques, UMR 8229. CNRS, Sorbonne Université, 75231 Paris Cedex 05, France;* orcid.org/0000-0002-8016-4747

Daniel Meyer − *ICSM, CEA, Univ Montpellier, CNRS, ENSCM, 30207 Marcoule, France*

Complete contact information is available at: https://pubs.acs.org/10.1021/acsaem.3c00447

Author Contributions

G.G. and B.M. contributed equally.

Notes

The authors declare no competing financial interest.

■ ACKNOWLEDGMENTS

Authors would like to thank the CEA (FOCUS CO_2 project) and the University of Montpellier for financial support.

■ REFERENCES

(1) Yaghi, O. M.; O'Keeffe, M.; Ockwig, N. W.; Chae, H. K.; Eddaoudi, M.; Kim, J. Reticular Synthesis and the Design of New Materials. *Nature* **2003**, *423* (6941), 705−714.

(2) Kitagawa, S.; Kitaura, R.; Noro, S. Functional Porous Coordination Polymers. *Angew. Chem., Int. Ed.* **2004**, *43* (18), 2334−2375.

(3) Janiak, C.; Vieth, J. K. MOFs, MILs and More: Concepts, Properties and Applications for Porous Coordination Networks (PCNs). *New J. Chem.* **2010**, *34* (11), 2366.

(4) Tranchemontagne, D. J.; Park, K. S.; Furukawa, H.; Eckert, J.; Knobler, C. B.; Yaghi, O. M. Hydrogen Storage in New Metal−Organic Frameworks. *J. Phys. Chem. C* **2012**, *116* (24), 13143−13151.

(5) Gonzalez, M. I.; Bloch, E. D.; Mason, J. A.; Teat, S. J.; Long, J. R. Single-Crystal-to-Single-Crystal Metalation of a Metal−Organic Framework: A Route toward Structurally Well-Defined Catalysts. *Inorg. Chem.* **2015**, *54* (6), 2995−3005.

(6) Carboni, M.; Abney, C. W.; Liu, S.; Lin, W. Highly Porous and Stable Metal−Organic Frameworks for Uranium Extraction. *Chem. Sci.* **2013**, *4* (6), 2396.

(7) Li, J.-R.; Sculley, J.; Zhou, H.-C. Metal−Organic Frameworks for Separations. *Chem. Rev.* **2012**, *112* (2), 869−932.

(8) Horcajada, P.; Gref, R.; Baati, T.; Allan, P. K.; Maurin, G.; Couvreur, P.; Férey, G.; Morris, R. E.; Serre, C. Metal−Organic Frameworks in Biomedicine. *Chem. Rev.* **2012**, *112* (2), 1232−1268.
(9) Taylor-Pashow, K. M. L.; Della Rocca, J.; Xie, Z.; Tran, S.; Lin, W. Postsynthetic Modifications of Iron-Carboxylate Nanoscale Metal−Organic Frameworks for Imaging and Drug Delivery. *J. Am. Chem. Soc.* **2009**, *131* (40), 14261−14263.
(10) Shen, L.; Liang, R.; Wu, L. Strategies for Engineering Metal-Organic Frameworks as Efficient Photocatalysts. *Chin. J. Catal.* **2015**, *36* (12), 2071−2088.
(11) Navarro Amador, R.; Carboni, M.; Meyer, D. Sorption and Photodegradation under Visible Light Irradiation of an Organic Pollutant by a Heterogeneous UiO-67−Ru−Ti MOF Obtained by Post-Synthetic Exchange. *RSC Adv.* **2017**, *7* (1), 195−200.
(12) Wang, L.; Jin, P.; Duan, S.; Huang, J.; She, H.; Wang, Q.; An, T. Accelerated Fenton-like Kinetics by Visible-Light-Driven Catalysis over Iron(III) Porphyrin Functionalized Zirconium MOF: Effective Promotion on the Degradation of Organic Contaminants. *Environ. Sci. Nano* **2019**, *6* (8), 2652−2661.
(13) Sharma, N.; Dey, A. K.; Sathe, R. Y.; Kumar, A.; Krishnan, V.; Kumar, T. J. D.; Nagaraja, C. M. Highly Efficient Visible-Light-Driven Reduction of Cr(VI) from Water by Porphyrin-Based Metal−Organic Frameworks: Effect of Band Gap Engineering on the Photocatalytic Activity. *Catal. Sci. Technol.* **2020**, *10* (22), 7724−7733.
(14) Han, B.; Ou, X.; Zhong, Z.; Liang, S.; Yan, X.; Deng, H.; Lin, Z. Photoconversion of Anthropogenic CO2 into Tunable Syngas over Industrial Wastes Derived Metal-Organic Frameworks. *Appl. Catal. B Environ.* **2021**, *283*, 119594.
(15) Wu, S.; Xu, Y.; Liu, M.; Li, X.; Zhang, X. Preparation of ZIF-8 Nanoparticle-Decorated Zn2GeO4 Nanorods with High Photocatalytic Performance for Chromium (VI) Reduction. *DESALINATION WATER Treat.* **2018**, *106*, 200−208.
(16) Ding, J.; Chen, M.; Du, X.; Shang, R.; Xia, M.; Hu, J.; Zhong, Q. Visible-Light-Driven Photoreduction of CO2 to CH4 with H2O Over Amine-Functionalized MIL-125(Ti). *Catal. Lett.* **2019**, *149* (12), 3287−3295.
(17) Bai, Y.; Dou, Y.; Xie, L.-H.; Rutledge, W.; Li, J.-R.; Zhou, H.-C. Zr-Based Metal−Organic Frameworks: Design, Synthesis, Structure, and Applications. *Chem. Soc. Rev.* **2016**, *45* (8), 2327−2367.
(18) Wang, J.-L.; Wang, C.; Lin, W. Metal−Organic Frameworks for Light Harvesting and Photocatalysis. *ACS Catal.* **2012**, *2* (12), 2630−2640.
(19) Maza, W. A.; Morris, A. J. Photophysical Characterization of a Ruthenium(II) Tris(2,2′-Bipyridine)-Doped Zirconium UiO-67 Metal−Organic Framework. *J. Phys. Chem. C* **2014**, *118*, 8803−8817.
(20) Wang, C.; Xie, Z.; deKrafft, K. E.; Lin, W. Doping Metal−Organic Frameworks for Water Oxidation, Carbon Dioxide Reduction, and Organic Photocatalysis. *J. Am. Chem. Soc.* **2011**, *133* (34), 13445−13454.
(21) Cohen, S. M. Postsynthetic Methods for the Functionalization of Metal−Organic Frameworks. *Chem. Rev.* **2012**, *112* (2), 970−1000.
(22) Chen, X.-H.; Wei, Q.; Hong, J.-D.; Xu, R.; Zhou, T.-H. Bifunctional Metal−Organic Frameworks toward Photocatalytic CO2 Reduction by Post-Synthetic Ligand Exchange. *Rare Met.* **2019**, *38* (5), 413−419.
(23) Li, J.; Huang, J.-Y.; Meng, Y.-X.; Li, L.; Zhang, L.-L.; Jiang, H.-L. Zr- and Ti-based metal−organic frameworks: synthesis, structures and catalytic applications. *Chem. Commun.* **2023**, *59*, 2541−2559.
(24) Wang, A.; Zhou, Y.; Wang, Z.; Chen, M.; Sun, L.; Liu, X. Titanium Incorporated with UiO-66(Zr)-Type Metal−Organic Framework (MOF) for Photocatalytic Application. *RSC Adv.* **2016**, *6* (5), 3671−3679.
(25) Sun, D.; Liu, W.; Qiu, M.; Zhang, Y.; Li, Z. Introduction of a mediator for enhancing photocatalytic performance via post-synthetic metal exchange in metal−organic frameworks (MOFs). *Chem. Commun.* **2015**, *51*, 2056−2059.
(26) Sun, D.; Liu, W.; Qiu, M.; Zhang, Y.; Li, Z. Correction: Introduction of a mediator for enhancing photocatalytic performance via post-synthetic metal exchange in metal−organic frameworks (MOFs). *Chem. Commun.* **2015**, *51*, 10765−10765.
(27) Lee, Y.; Kim, S.; Kang, J. K.; Cohen, S. M. Photocatalytic CO2 reduction by a mixed metal (Zr/Ti), mixed ligand metal−organic framework under visible light irradiation. *Chem. Commun.* **2015**, *51*, 5735−5738.
(28) Denny, M. S.; Parent, L. R.; Patterson, J. P.; Meena, S. K.; Pham, H.; Abellan, P.; Ramasse, Q. M.; Paesani, F.; Gianneschi, N. C.; Cohen, S. M. Transmission Electron Microscopy Reveals Deposition of Metal Oxide Coatings onto Metal−Organic Frameworks. *J. Am. Chem. Soc.* **2018**, *140* (4), 1348−1357.
(29) Santaclara, J. G.; Olivos-Suarez, A. I.; Gonzalez-Nelson, A.; Osadchii, D.; Nasalevich, M. A.; van der Veen, M. A.; Kapteijn, F.; Sheveleva, A. M.; Veber, S. L.; Fedin, M. V.; Murray, A. T.; Hendon, C. H.; Walsh, A.; Gascon, J. Revisiting the Incorporation of Ti(IV) in UiO-type Metal−Organic Frameworks: Metal Exchange versus Grafting and Their Implications on Photocatalysis. *Chem. Mater.* **2017**, *29* (21), 8963−8967.
(30) Walsh, A.; Butler, K. T.; Hendon, C. H. Chemical principles for electroactive metal−organic frameworks. *MRS Bull.* **2016**, *41*, 870−876.
(31) Benck, J. D.; Pinaud, B. A.; Gorlin, Y.; Jaramillo, T. F. Substrate Selection for Fundamental Studies of Electrocatalysts and Photoelectrodes: Inert Potential Windows in Acidic, Neutral, and Basic Electrolyte. *PLoS One* **2014**, *9* (10), e107942.
(32) Crivello, C.; Sevim, S.; Graniel, O.; Franco, C.; Pané, S.; Puigmarti-Luis, J.; Muñoz-Rojas, D. Advanced technologies for the fabrication of MOF thin films. *Materials Horizons* **2021**, *8*, 168−178.
(33) Shekhah, O.; Liu, J.; Fischer, R. A.; Wöll, C. MOF thin films: existing and future applications. *Chem. Soc. Rev.* **2011**, *40*, 1081−1106.
(34) Genesio, G.; Maynadié, J.; Carboni, M.; Meyer, D. Recent Status on MOF Thin Films on Transparent Conductive Oxides Substrates (ITO or FTO). *New J. Chem.* **2018**, *42*, 2351−2363.
(35) Shi, X.; Shan, Y.; Du, M.; Pang, H. Synthesis and application of metal-organic framework films. *Coord. Chem. Rev.* **2021**, *444*, 214060.
(36) Maza, W. A.; Ahrenholtz, S. R.; Epley, C. C.; Day, C. S.; Morris, A. J. Solvothermal Growth and Photophysical Characterization of a Ruthenium(II) Tris(2,2′-Bipyridine)-Doped Zirconium UiO-67 Metal Organic Framework Thin Film. *J. Phys. Chem. C* **2014**, *118* (26), 14200−14210.
(37) Maza, W. A.; Haring, A. J.; Ahrenholtz, S. R.; Epley, C. C.; Lin, S. Y.; Morris, A. J. Ruthenium(II)-Polypyridyl Zirconium(IV) Metal−Organic Frameworks as a New Class of Sensitized Solar Cells. *Chem. Sci.* **2016**, *7* (1), 719−727.
(38) Lin, S.; Pineda-Galvan, Y.; Maza, W. A.; Epley, C. C.; Zhu, J.; Kessinger, M. C.; Pushkar, Y.; Morris, A. J. Electrochemical Water Oxidation by a Catalyst-Modified Metal-Organic Framework Thin Film. *ChemSusChem* **2017**, *10* (3), 514−522.
(39) Johnson, B. A.; Bhunia, A.; Ott, S. Electrocatalytic Water Oxidation by a Molecular Catalyst Incorporated into a Metal−Organic Framework Thin Film. *Dalton Trans* **2017**, *46* (5), 1382−1388.
(40) Zhu, L.; Lu, Q.; Lv, L.; Wang, Y.; Hu, Y.; Deng, Z.; Lou, Z.; Hou, Y.; Teng, F. Ligand-free rutile and anatase TiO_2 nanocrystals as electron extraction layers for high performance inverted polymer solar cells. *RSC Adv.* **2017**, *7*, 20084.
(41) Paille, G.; Gomez-Mingot, M.; Roch-Marchal, C.; Haouas, M.; Benseghir, Y.; Pino, T.; Ha-Thi, H.-T.; Landrot, G.; Mialane, P.; Fontecave, M.; Dolbecq, A.; Mellot-Draznieks, C. Thin Films of Fully Noble Metal-Free POM@MOF for Photocatalytic Water Oxidation. *ACS Appl. Mater. Interfaces* **2019**, *11* (51), 47837−47845.

https://doi.org/10.1021/acsaem.3c00447
ACS Appl. Energy Mater. 2023, 6, 9188−9195